BCG immunotherapy inhibits cancer progression by promoting the M1 macrophage differentiation of THP-1 cells via the Rb/E2F1 pathway in cervical carcinoma

LIMIN LIU[1], WENJUAN SHI[1], XIAO XIAO[2], XUEMEI WU[1], HAIYAN HU[1], SHIXIN YUAN[3], KAI LIU[1] and ZHIHUA LIU[1]

Departments of [1]Gynecology and [2]Obstetrics, [3]Institute of Maternal and Child Medicine, Affiliated Shenzhen Maternity and Child Healthcare Hospital, Southern Medical University, Shenzhen, Guangdong 518028, P.R. China

Received October 31, 2020; Accepted July 19, 2021

DOI: 10.3892/or.2021.8196

Abstract. Bacillus Calmette-Guérin (BCG) immunotherapy increases macrophage polarization toward M1-type macrophages. In the present study, to identify the M1/M2 marker genes in the carcinogenesis and progression of cervical cancer, the microarray datasets GSE9750 and GSE7803 were downloaded from The Cancer Genome Atlas (TCGA), Gene Expression Omnibus (GEO) and the University of California Santa Cruz (UCSC) Xena browser. Survival analysis revealed that M1 markers (IL-12) were involved in anti-tumour progression, and M2 markers (IL-10) were involved in the carcinogenesis and invasion of cervical cancer. The expression of M1 markers (IL-12, inducible nitric oxide synthase and CD80) and M2 markers (IL-10 and arginase) was examined to determine whether BCG affects the polarization of macrophages and to elucidate the underlying mechanisms. The results revealed that BCG promoted macrophage polarization towards the M1 phenotype and enhanced the transition of M2 to M1 macrophages. The results also revealed that polarized M1 macrophages induced by BCG decreased the protein expression of phosphorylated (p-)retinoblastoma (Rb)/E2F transcription factor 1 (E2F1), inhibited the proliferation and promoted the apoptosis of HeLa cells. On the whole, these results demonstrated that BCG promoted the anti-tumour progression of M1 macrophages and inhibited the pro-tumour activation of M2 macrophages via the Rb/E2F1 signalling pathway in HeLa cells. This suggests the possibility of a direct translation of this combination strategy to clinical practice for the treatment of cervical cancer.

Correspondence to: Professor Zhihua Liu or Professor Haiyan Hu, Department of Gynecology, Affiliated Shenzhen Maternity and Child Healthcare Hospital, Southern Medical University, 2004 Hongli Road, Futian, Shenzhen, Guangdong 518028, P.R. China
E-mail: drzhliu@163.com
E-mail: 2419959031@qq.com

Key words: Bacillus Calmette-Guérin, cervical cancer, M1 macrophages, tumour-associated macrophages, cell proliferation, cell apoptosis

Introduction

Cervical cancer is the fourth most common type of malignant tumour affecting women worldwide (1). Although the mortality rate of patients with cervical cancer has decreased in recent decades due to radical surgery and chemoradiotherapy, the treatment of this type of cancer remains an immense global challenge due to its recurrence, invasion and metastasis rate (2). Therefore, effective prevention and treatment strategies for cervical cancer are required, particularly immunotherapy targeting its pathogenesis.

Mycobacterium bovis Bacillus Calmette-Guérin (BCG) is a live attenuated bovine tuberculosis vaccine that is the first choice for intravesical treatment, and it is the gold standard for the immunotherapy of superficial bladder cancer (3-5). Genitourinary tumours, such as bladder cancer (6) and benign diseases, including condyloma acuminatum and cervical genital warts, are closely related to human papillomavirus (HPV) infection (7-9). Clinical studies have established that BCG immunotherapy exerts a specific effect on genital warts of the genitourinary system (7,9). R also identified a certain therapeutic effect on cervical condyloma acuminate with the local injection of BCG (8). However, whether BCG intervention is an effective treatment for cervical cancer remains unknown. Patients with cervical cancer often have severe cellular immune dysfunction. BCG has been shown to exert a significant therapeutic effect against cervical intraepithelial neoplasia (CIN II-III in combination with interferon (IFN) and improves the cellular immune function of patients with tumours (10). BCG-activated peripheral blood mononuclear cells also exert a significant killing effect on high-risk HPV-infected HeLa cells (11). Therefore, BCG intervention for cervical cancer holds promise as a novel immunotherapy method.

The mechanism of BCG immunotherapy is attributed to a local non-specific immune response that kills tumour cells: The interaction of inflammation and cancer (12). Tumour-associated

macrophages (TAMs) play a key role in tumour immunosuppression and progression (13). Macrophages are differentiated from bone marrow-derived monocytes and have a high heterogeneity and plasticity, exerting a number of effects on the microenvironment (14,15). Macrophages are often classified as the classically activated M1 type and alternatively activated M2 type based on cell functions. M1 macrophages are primarily stimulated by lipopolysaccharide (LPS) or IFN-γ (16) and possess high antigen-presenting capabilities (17), which are characterized by the high secretion of pro-inflammatory cytokines, such as IL-6, IL-12, IL-23 and TNF-α (18), to promote a Th1 response, and microbicidal and tumoricidal activities (19). M2 macrophages are polarized via IL-4, IL-10, and IL-13 and exhibit a weak antigen-presenting ability (20). These cells are known as the 'repair' macrophages and are associated with parasite containment, tissue remodelling, debris elimination, immune tolerance and regulatory functions, which ultimately lead to the immune escape of tumour cells (21). The present study used LPS and IFN-γ to polarize M1 macrophages, and M2 macrophages were polarized with IL-4.

In the present study, microarray datasets were downloaded from the Gene Expression Omnibus (GEO) and The Cancer Genome Atlas (TCGA) and the differentially expressed genes (DEGs) and functional pathways were analysed between cervical cancer tissues, high-grade squamous intraepithelial lesion (HSIL) of the cervix tissues and normal cervical tissues. Gene Ontology (GO) and Kyoto Encyclopedia of Genes and Genomes (KEGG) pathway enrichment analyses and protein-protein interaction (PPI) network analyses were used to elucidate molecular mechanisms underlying the carcinogenesis and progression of cervical cancer. Survival analysis revealed that M1 markers played an anti-tumour role, and M2 markers were involved in the carcinogenesis and invasion of cervical cancer.

Persistent infection with high-risk HPV is a major risk factor for cervical cancer (22). The majority of cervical cancers are associated with a high risk of HPV infection, and HPV16 and 18 are associated with ~70% of all cervical cancers (23). Immunotherapy stimulates the regression of certain virus-associated epithelial malignancies, such as HPV-induced cancers in the cervix (24), head and neck (25) and anus (26). Viral oncoproteins from tumours with HPV-positive expression are latent candidate tumour degradation antigens as these proteins are immunologically foreign and are essentially expressed by cancer cells (27,28). However, evidence supporting their role in immunotherapy-mediated tumour degradation is limited.

In the present study, the association of IL-12 and IL-10 with survival was examined and the survival-based cell cycle and p53 signalling pathways in cervical cancer were identified using TCGA and GEO databases. Furthermore, the effects and molecular mechanisms of action of BCG on the polarization of M1 and M2 macrophages, and the regulation of the p53/retinoblastoma (Rb)/E2F transcription factor 1 (E2F1) pathway in HeLa cervical cancer cells were investigated in order to provide a theoretical basis for the clinical immunotherapy of cervical cancer.

Materials and methods

Cervical cancer datasets and pre-processing. Cervical cancer gene expression data that were publicly available and reported in full clinical annotation were systematically searched. The microarray datasets, GSE9750 and GSE7803 (Affymetrix GPL96 platform, Affymetrix Human Genome U133A Array), and TCGA-cervical squamous cell carcinoma (CESC) were downloaded from the GEO database (http://www.ncbi.nlm.nih.gov/geo) and UCSC Xena browser (https://xenabrowser.net/datapages/). The GSE9750 dataset contains 24 normal cervical tissue samples and 28 cervical cancer tissue samples. The GSE7803 dataset contains 10 normal cervix tissue samples, 7 HSIL tissue samples and 21 cervical cancer tissue samples. The DEGs, with log fold change (FC) >3 and adj. P-value <0.01, in the mRNA expression profiling sets, GSE9750 and GSE7803, were selected with GEO2R (http://www.ncbi.nlm.nih.gov/geo/geo2r).

Survival analysis. GEPIA is a recently published analysis tool containing the RNA sequencing expression data of 8,587 normal samples and 9,736 tumour samples (http://gepia.cancer-pku.cn). GEPIA provides differential mRNA expression analysis of tumour/normal tissues and pathological stages or grades for analysis, patient survival analysis and correlation analysis (29). The cut-off P-value was 0.05. The association between mRNA expression and overall survival (OS), or disease-free survival (DFS) was determined using the 'Cox PH Model' with the Kaplan-Meier survival plot. The survival curves of samples with high and low gene expression were compared using the log-rank test.

UALCAN (http://ualcan.path.uab.edu) is a comprehensive web resource based on the TCGA that includes the clinical data of 31 cancer types and the MET500 cohort database (30). In the present study, UALCAN was used to analyse the mRNA expression levels of IL-12 and IL-10 in primary CESC tissues and their association with pathological stage and survival. The association between mRNA expression and pathological stage was determined using an unpaired Student's t-test (between 2 groups) or one-way analysis of variance (ANOVA) (between multiple groups) followed by the LSD or Tukey's multiple comparisons post hoc test. The survival analysis of the UALCAN survival curves was performed in the same manner as that for the GEPIA data. The cut-off P-value was 0.05.

Functional and pathway enrichment analyses of DEGs. The functions of 939 DEGs in the GSE7803/9750 cervical cancer samples were analysed with GO and KEGG in the Database for Annotation, Visualization, and Integrated Discovery (DAVID) (https://david.ncifcrf.gov/summary.jsp) (31). GO enrichment analysis was used to predict the biological processes of 939 DEGs, and KEGG analysis was used to define the pathways related to the 939 DEGs in the GSE7803/9750 CESC samples.

PPI network. The PPI network was obtained by using the Search Tool for the Retrieval of Interacting Genes (STRING) (http://string-db.org) database (32). In the present study, PPI network analysis of M1/M2 markers and Rb/E2F1 pathway proteins was conducted to examine their interactions using the STRING database. An interaction score >0.4 was considered statistically significant.

THP-1 cell culture and macrophage differentiation. Human monocyte THP-1 cells (ATCC® TIB-202TM) were

Table I. Primer sequences used for RT-qPCR.

IL-10	Forward primer: CACTGCTCTGTTGCCTGGTC
	Reverse primer: GAAGCATGTTAGGCAGGTTGC
IL-12	Forward primer: GGACCTTGGACCAGAGCAGT
	Reverse primer: GGCTTAGAACCTCGCCTCCT
ARG	Forward primer: TTGGCTTGAGAGACGTGGAC
	Reverse primer: CCATCACCTTGCCAATTCCT
iNOS	Forward primer: GAGCCAGGCCACCTCTATGT
	Reverse primer: GTCCTCGACCTGCTCCTCAT
GAPDH	Forward primer: CGGAGTCAACGGATTTGGTCGTAT
	Reverse primer: AGCCTTCTCCATGGTGGTGAAGAC

iNOS, inducible nitric oxide synthase; ARG, arginase.

maintained at 37˚C in a humidified incubator with 5% CO_2. Cells were cultured in Roswell Park Memorial Institute medium (RPMI-1640; Invitrogen; Thermo Fisher Scientific, Inc.) supplemented with 10% heat-inactivated foetal bovine serum (FBS Natocor), 100 U/ml penicillin and 100 μg/ml streptomycin (all from Invitrogen; Thermo Fisher Scientific, Inc.). Resting macrophages (M0) were differentiated from THP-1 monocytes with 5-100 ng/ml phorbol 12-myristate-13 acetate (PMA, P8139, Sigma-Aldrich; Merck KGaA) for 24 h, and 10 ng/ml PMA was considered optimal. M1 macrophages were polarized with 5-40 ng/ml IFN-γ (11725-HNAS; Sino Biological Inc.) and 20-100 ng/ml LPS (L2880; Sigma-Aldrich; Merck KGaA), and 20 ng/ml IFN-γ and 100 ng/ml LPS were considered optimal. M2 macrophages were obtained by incubation with 5-40 ng/ml IL-4 (#20004; PeproTech, Inc.) at 37˚C for 48 h, and 10 ng/ml IL-4 was considered optimal. M1/M2 macrophages were further induced with BCG (Shanghai Institute of Biological Products, China) at various concentrations (0.2-40 μg/ml) for 48 h.

Enzyme-linked immunosorbent assay (ELISA). Macrophage supernatants were collected from the THP-1/M0/M1/M2 groups. After 48 h, the levels of IL-10 (ELISA kit, 88-7106; eBioscience) and IL-12 (Elisa Kit, 88-7929; eBioscience) of serum samples were assayed using ELISA multiplex kits according to the manufacturer's protocol.

Reverse transcription-quantitative PCR (RT-qPCR). RNA was extracted using TRIzol® reagent (Invitrogen; Thermo Fisher Scientific, Inc.), and RNA purity and concentration were determined using a UV spectrophotometer. RNA was reverse transcribed into cDNA using a PrimeScriptTM^{RT} reagent kit (Takara Bio, Inc.). According to the SYBR® Premix Ex Taq (Takara Bio, Inc.) manufacturer's protocol, amplification was performed using a CFX96TM Real-Time PCR Detection System (Bio-Rad Laboratories, Inc.). The standard reaction conditions were 95˚C for 30 sec; and 95˚C for 5 sec and 60˚C for 30 sec for 40 cycles. Relative quantification was performed using the $2^{-\Delta\Delta Cq}$ method (33). The Cq value was automatically analysed based on the amplification curve. The $2^{-\Delta\Delta Cq}$ value represents the expression level of a target gene in each group relative to the expression level of the internal reference gene (34). GAPDH served as the control gene for normalization. All the reactions were performed in triplicate. The primer sequences are listed in Table I.

Western blot analysis. THP-1/macrophages and cervical carcinoma HeLa cells (Shanghai Institutes for Biological Sciences) were co-cultured in a separate chamber at 37˚C in a humidified incubator with 5% CO_2 for 96 h. Total proteins were extracted from the HeLa cells using lysis buffer (Beyotime Institute of Biotechnology). The protein concentration was determined using the BCA-100 protein quantitation method (Nanjing KeyGen Biotech Co., Ltd.). An 8-12% separation gel and a 5% stacking gel were prepared for electrophoresis. The separated proteins (20 μg) were transferred to a PVDF membrane (EMD Millipore) with the wet transfer method. The membranes were blocked with BSA (Beijing Solarbio Science & Technology Co., Ltd.) for 1 h, and anti-p53 (1:1,000, cat. no. 2524) anti-phosphorylated (p-) Rb (1:1,000, cat. no. 9313), anti-E2F1(1:1,000, cat. no. 3742), anti-ARG (1:1,000, cat. no. 93668) anti-GAPDH antibodies (1:1,000, cat. no. D16H11) (all from Cell Signaling Technology, Inc.) and anti-iNOS (1:500, MAB9502; R&D Systems, Inc.) were added overnight at 4˚C. The membranes were washed with 1X Tris-buffered saline-Tween (TBST, Beijing Solarbio Science & Technology Co., Ltd.) for 5 min (3 times). A goat anti-rabbit antibody and goat anti-mouse antibody (H + L; Invitrogen; Thermo Fisher Scientific, Inc.) were used as the secondary antibodies. The membranes were incubated with the secondary antibodies (anti-mouse IgG, 1:2,000, cat. no. 7076; Cell Signaling Technology, Inc.; anti-rabbit IgG, 1:2,000, cat. no. 7074; Cell Signaling Technology, Inc.) at room temperature for 1-2 h and washed with 1X TBST for 5 min (3 times). The membranes were incubated with enhanced chemiluminescence (ECL) substrate (EMD Millipore), and the blots were developed on an ultrasensitive chemiluminescence imaging system (Bio-Rad Laboratories, Inc.). All the reactions were performed in triplicate. GAPDH served as a control protein to quantify the expression of target proteins using Image Lab software 4.0 (Bio-Rad Laboratories, Inc.).

Flow cytometric analysis. Cells were separated with trypsin and washed with PBS Gibco; Thermo Fisher Scientific, Inc.).

The cells were cultured with a PE-conjugated anti-mouse CD80 antibody (cat. no. 561134; BD Biosciences) for 20 min at room temperature and analysed on a FACS-Verse flow cytometer (BD Biosciences). The data were analysed using FlowJo software 7.6 (BD Biosciences).

For the cell cycle assay, the cells were isolated with trypsin and suspended in PBS. The cells were incubated in pre-cooled 70% ethanol, and the ethanol was discarded following centrifugation at room temperature at 800 x g for 6 min. The cells were suspended in PBS. Propidium iodide (PI, 450 μl)/RNase (50 μl) staining buffer (BD Pharmingen; BD Biosciences) was added, and the reaction was performed in the dark at room temperature for 30 min. A FACS flow cytometer was used (FACS Verse; BD Biosciences).

For the Cell apoptosis assay: Cells were digested with trypsin without ethylenediaminetetraacetic acid (EDTA). The cells were suspended in PBS. To each sample, 100 μl of 1X binding buffer, 5 μl of FITC-Annexin V (eBioscience; Thermo Fisher Scientific, Inc.) and 10 μl PI (eBioscience; Thermo Fisher Scientific, Inc.) were added in the dark at room temperature for 15 min and mixed with 400 μl PBS. A FACS flow cytometer was used (FACS Verse; BD Biosciences).

Statistical analysis. Statistical analyses were performed using SPSS 20.0 statistical software (IBM Corp.). Statistical analyses were performed using an unpaired Student's t-test (between 2 groups) or one-way analysis of variance (ANOVA) (between multiple groups) followed by LSD or Tukey's post hoc multiple comparisons. Measurement data are expressed as the mean ± standard error of the mean (SEM) from one representative experiment of three independent experiments. P<0.05 was considered to indicate a statistically significant difference. Figures were generated using GraphPad Prism 7 (GraphPad Software, Inc.) and Adobe illustrator CS6 (Adobe Systems, Inc.).

Results

Aberrant expression of IL-12 and IL-10 in patients with CESC. To examine the distinct prognostic and potential therapeutic value of M1/M2 markers in patients with CESC, the mRNA expression levels of IL-12 and IL-10 were analysed in primary CESC tissues, and their association with pathological stages were assessed with UALCAN and the GEO. IL-12 mRNA expression was slightly higher in CESC tissues than in normal tissues (P<0.05) (Fig. 1A) and tended to be weakly expressed in patients with more advanced stages according to UALCAN (Fig. 1B). The mRNA expression of IL-10 was significantly higher in CESC tissues than in normal tissues according to UALCAN (P<0.001) (Fig. 1C). IL-10 expression was markedly associated with CESC stages and tended to be more highly expressed in patients with more advanced stages of the disease (Fig. 1D).

Prognostic value of IL-12 and IL-10 in patients with CESC. To evaluate the role of IL-12 and IL-10 in the progression of CESC, the associations of IL-12 and IL-10 expression and the clinical outcomes of patients were assessed using GEPIA and UALCAN. The results of overall survival (OS) and disease-free survival (DFS) are presented in Fig. 2. It was found that high transcriptional levels of IL-12 were significantly associated with a prolonged OS in patients with CESC (GEPIA, P<0.05; UALCAN, P<0.001) (Fig. 2A and C). High transcriptional levels of IL-10 were significantly associated with DFS according to GEPIA (P<0.001) (Fig. 2B and D).

Identification, KEGG and GO enrichment analyses of DEGs in GSE7803/9750. DEGs (2,049 in GSE7803 and 3,268 in GSE9750) were identified following the standardization of the microarray results. Among the two datasets, 939 genes overlapped, as displayed in the Venn diagram in Fig. 3A. The mRNA expression of IL-10 was also significantly upregulated in CESC tissues compared with normal and HSIL tissues from GSE7803 (P<0.05; P<0.001) (Fig. 3B). The mRNA expression of IL-12 was significantly downregulated in CESC tissues compared with normal tissues from GSE9750 (P<0.001) (Fig. 3C). The functional and pathway enrichment analyses of the DEGs were predicted with GO and KEGG in DAVID. It was found that GO: 0051301 (cell division), GO: 0000082 (G1/S transition of mitotic cell cycle), GO: 0008283 (cell proliferation), GO: 0007049 (cell cycle), GO: 1901796 (regulation of signal transduction by p53) and GO: 0006955 (immune response) were significantly enriched in DEGs in GSE7803/9750 (Table II). KEGG pathway analysis revealed that hsa04110 (cell cycle), hsa03030 (DNA replication), hsa03420 (nucleotide excision repair) and hsa04115 (p53 signalling pathway) were enriched in DEGs in GSE7803/9750 (Table II).

PPI network construction. The PPI network analysis of M1/M2 markers and RB/E2F1 pathway proteins was performed to examine the interactions between IL-12, IL-10, IL-4, CD80, ARG-1, NOS, p53, Rb and E2F1 using the STRING database. As was expected, the results revealed several nodes (12) and several edges (18) in the PPI network (Fig. 3D).

Characterization of macrophage polarization from THP-1 monocytes. M0 macrophages were differentiated from THP-1 monocytes using 5-100 ng/ml PMA in 6-well plates for 24 h. The hallmarks of macrophages were observed under a microscope as THP-1 cells became adherent from the suspension and spread. The results revealed that the optimal condition was 10 ng/ml PMA for M0 macrophage differentiation (Fig. 4A). M1 macrophages were obtained by incubating M0 macrophages with 5-40 ng/ml IFN-γ and 20-100 ng/ml LPS. M2 macrophages were induced with 5-40 ng/ml IL-4. The mRNA and protein expression of IL-10 revealed that 10 ng/ml IL-4 was the optimal concentration for M2 macrophage polarization (Fig. 4B and C). The mRNA and protein expression of IL-12 indicated that 20 ng/ml IFN-γ and 100 ng/ml LPS were optimal for M1 macrophage polarization (Fig. 4D-F).

THP-1 cells were differentiated into M0 macrophages with PMA for 24 h and further polarized toward M1/M2 phenotype macrophages with IFN-γ and LPS or IL-4 at the appropriate concentrations for 48 h. The results of RT-qPCR revealed that the M2 macrophages had a higher IL-10 mRNA expression than the M0/M1 macrophages (Fig. 5A), and IL-12 mRNA expression in M1 macrophages was significantly higher than that in M0/M2 macrophages (Fig. 5B). The FACS results demonstrated that M1 macrophages had higher CD80 protein expression than M0/M1 macrophages (Fig. 5C and D).

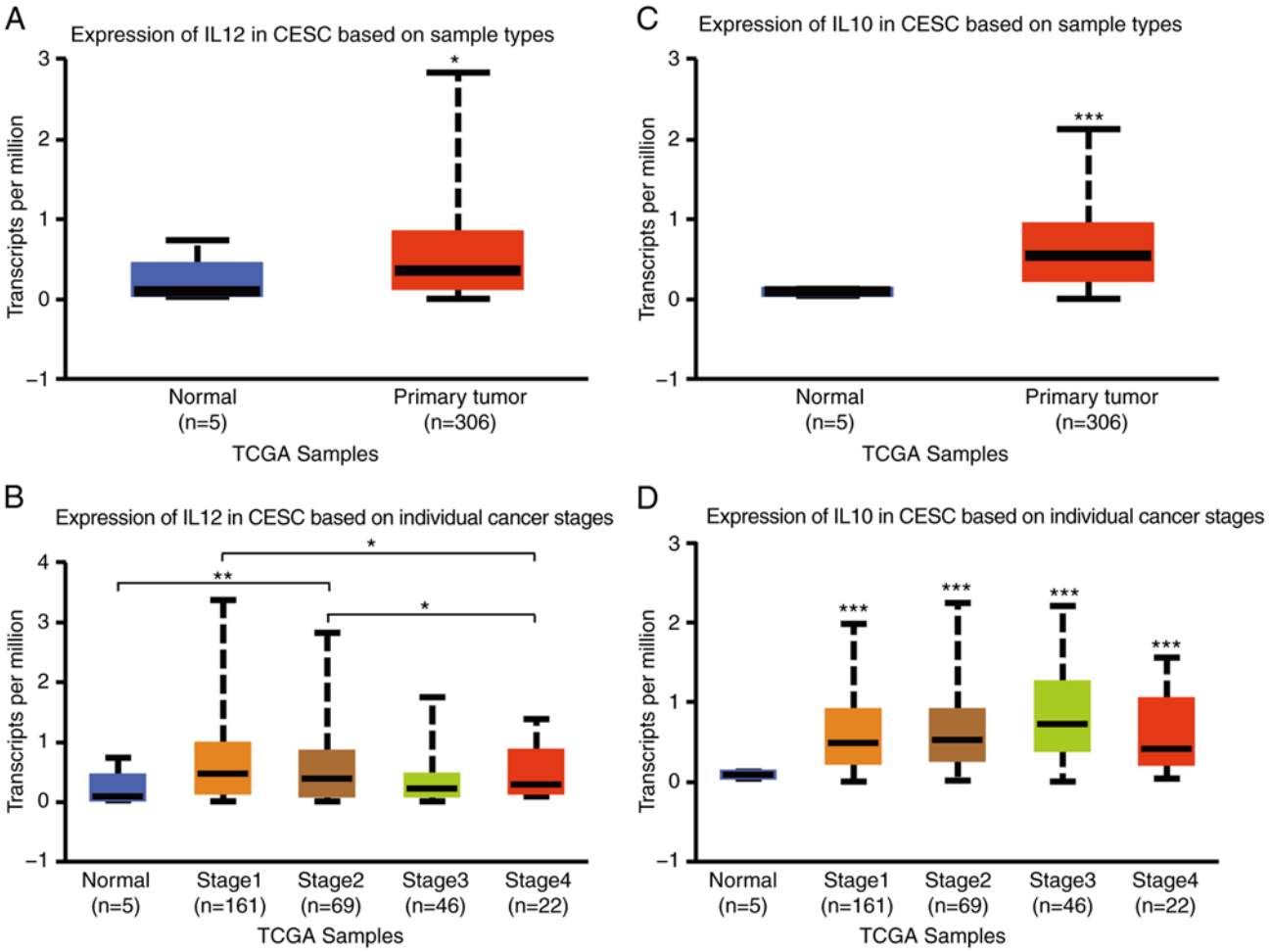

Figure 1. Association between the expression of IL-12 and IL-10 and tumour stage in CESC. (A) IL-12 mRNA expression in CESC tissues compared to normal tissues (*P<0.05). (B) IL-12 mRNA expression in CESC samples with tumour stages (*P<0.05, **P<0.01). (C) IL-10 mRNA expression in CESC tissues compared to normal tissues (***P<0.001). (D) IL-10 mRNA expression in CESC samples with tumour stages (***P<0.001, as compared with normal group). CESC, cervical squamous cell carcinoma.

The ELISA results demonstrated that the IL-10 levels in M2 macrophages were higher than those in M0/M1 macrophages (Fig. 5E); however, the IL-12 levels in M1 macrophages were higher than those in M0/M2 macrophages (Fig. 5F).

BCG promotes macrophage polarization toward the M1 phenotype and enhances the transition of M2 to M1 macrophages. To observe the effects of BCG on macrophage polarization, the M1/M2 macrophages were treated with various concentrations (0.2-40 μg/ml) of BCG for 48 h (35). The mRNA or protein expression of IL-12 and iNOS (M1 markers) steadily increased in the 0.2 to 20 μg/ml BCG-activated M1/M2 macrophage groups, particularly in the M1 macrophage group, and decreased in the 40 μg/ml BCG-activated M1 macrophage group, likely due to toxicity (Fig. 6A-C). The mRNA or protein expression levels of IL-10 and ARG (M2 markers) were inhibited in the 0.2-20 μg/ml BCG-activated M1/M2 macrophage groups, and the levels of these markers were particularly decreased in the M2 macrophage group. No significant differences in ARG expression were found between the 0.2-40 μg/ml BCG-activated M1 macrophage groups and the M1 macrophage group (Fig. 6D-F). These findings indicated that the 20 μg/ml BCG condition led to maximum activation.

BCG promotes the anti-tumour progression of M1 macrophages and inhibits the pro-tumour activation of M2 macrophages in HeLa cells. The effects of polarized macrophages induced by BCG on HeLa cell proliferation and apoptosis were further assessed. THP-1/macrophages and HeLa cells were co-cultured in a separate chamber for 96 h. Cell cycle analysis revealed that the M1 macrophages had an increased the proportion of cells in the G0/G1 phase, and the number of cells in the S phase was decreased in the HeLa cells compared with the THP-1/M0 macrophages. M2 macrophages exhibited a decreased number of cells in the G0/G1 phase and an increased proportion of cells in the S phase in HeLa cells compared with the THP-1/M0 macrophages. (Fig. 7A and B). Cell apoptosis analysis revealed that M1 macrophages increased the percentage of HeLa cells in early apoptosis, and BCG further increased the proportion of cells in early apoptosis compared with M2 macrophages without BCG (Fig. 7C and D).

Polarized macrophages induced by BCG affect HeLa cell proliferation via the Rb/E2F1 signalling pathway. The present study then investigated whether Rb/E2F1 expression in HeLa cells was influenced by BCG-induced M1/M2 macrophages.

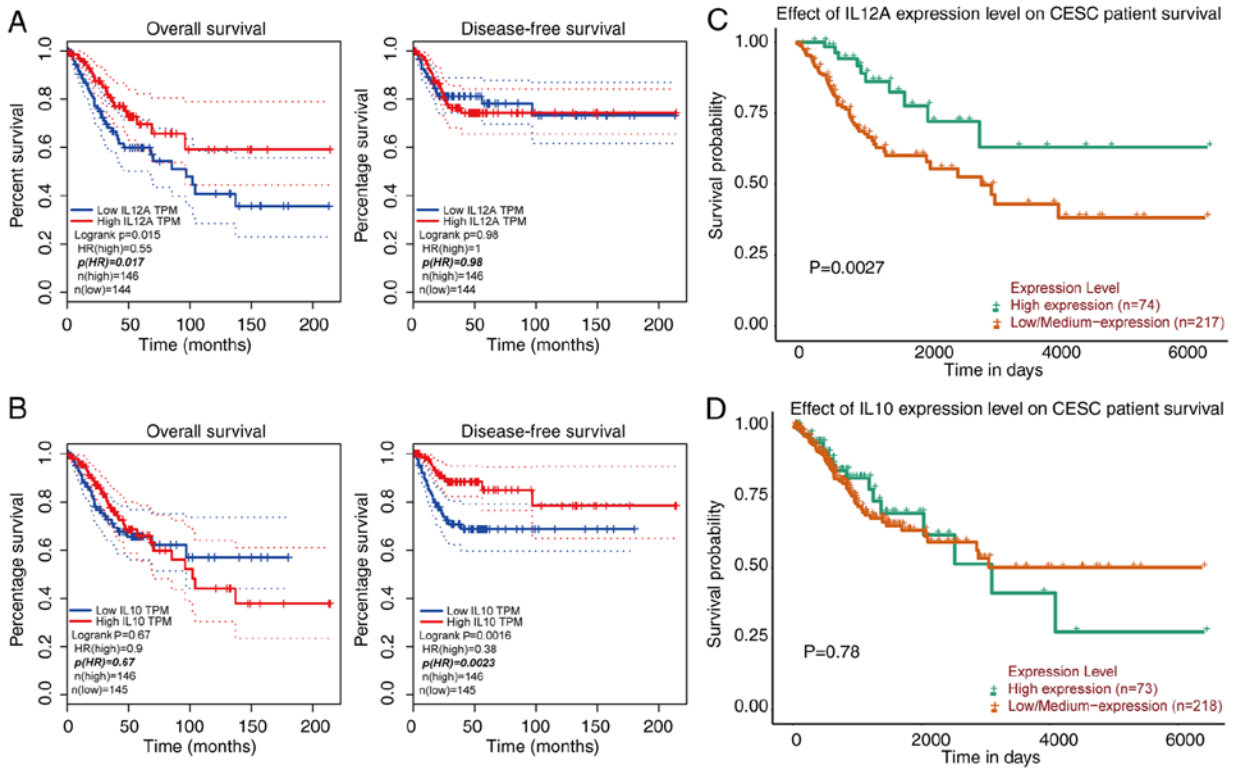

Figure 2. Prognostic value of IL-12 and IL-10 in CESC in the OS and DFS curves (GEPIA, UALCAN). (A) IL-12 mRNA expression in the OS and DFS curves in CESC (GEPIA). (B) IL-10 mRNA expression in the OS and DFS curves in CESC (GEPIA). (C) IL-12 mRNA expression in the OS curve in CESC (UALCAN). (D) IL-10 mRNA expression in the OS curve in CESC (UALCAN). CESC, Cervical squamous cell carcinoma; OS, overall survival; DFS, disease-free survival.

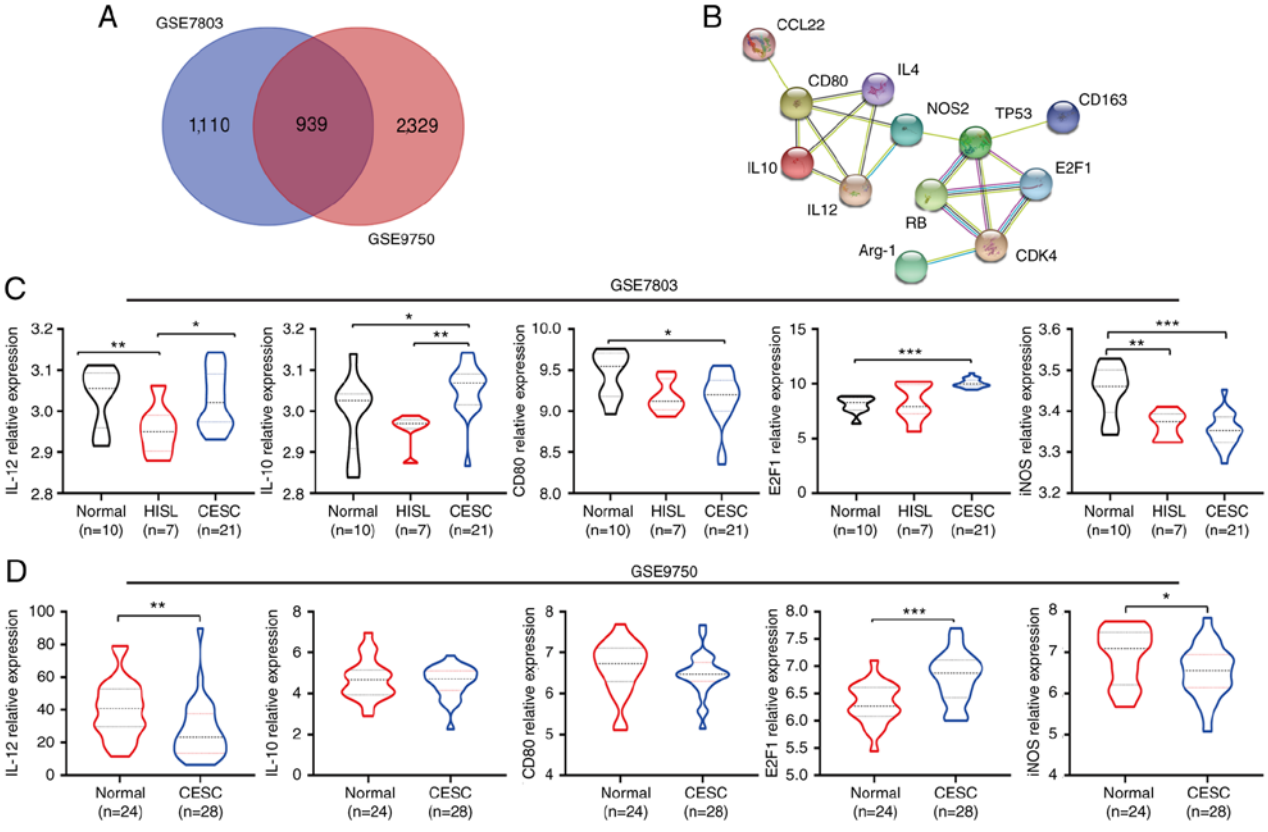

Figure 3. Venn diagram, PPI network and M1/M2 marker expression in the GSE7803 and GSE9750 datasets. (A) DEGs (log FC >3 and adj. P-value <0.01) were selected from the mRNA expression profiling sets GSE7803 and GSE9750. (B) PPI network of M1/M2 markers was constructed using the STRING database. (C) M1/M2 marker expression in the GSE7803 dataset (*P<0.05, **P<0.01 and ***P<0.001, compared between the groups). (D) M1/M2 marker expression in the GSE9750 dataset. PPI, protein-protein interaction; DEGs, differentially expressed genes (*P<0.05, **P<0.01 and ***P<0.001, compared between the groups).

Table II. GO and KEGG pathway enrichment analysis of DEGs in GSE 7803/9750 CESC samples.

Pathway ID	Description	Count in gene set	P-value
GO:0051301	Cell division	66	<0.001
GO:0006260	DNA replication	43	<0.001
GO:0000082	G1/S transition of mitotic cell cycle	31	<0.001
GO:0000086	G2/M transition of mitotic cell cycle	29	<0.001
GO:0008283	Cell proliferation	47	<0.001
GO:0007049	Cell cycle	26	<0.001
GO:1901796	Regulation of signal transduction by p53	18	<0.001
GO:0075733	Intracellular transport of virus	10	<0.001
GO:0006955	Immune response	34	<0.01
GO:0043066	Negative regulation of apoptotic process	36	<0.01
hsa04110	Cell cycle	34	<0.001
hsa03030	DNA replication	18	<0.001
hsa03420	Nucleotide excision repair	9	<0.01
hsa04115	p53 signalling pathway	10	<0.05

GO, Gene Ontology; KEGG, Kyoto Encyclopedia of Genes and Genomes; DEGs, differentially expressed genes.

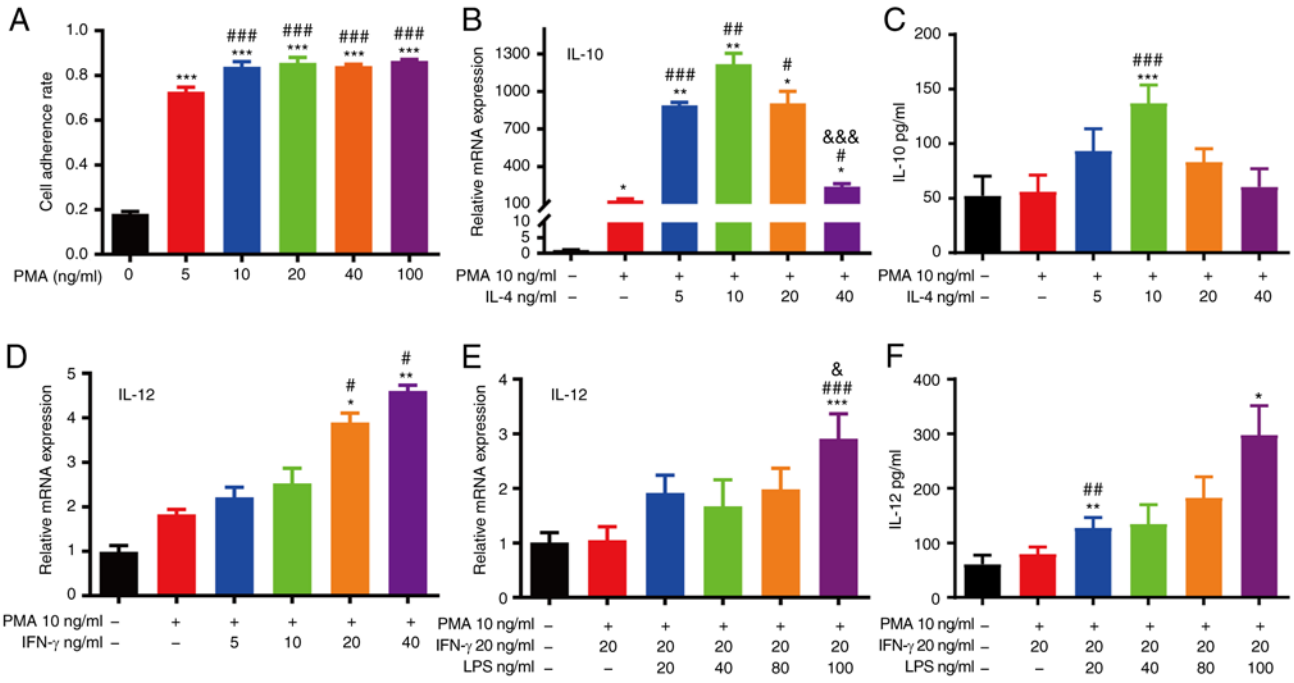

Figure 4. Differentiation of THP-1 monocytes into macrophages. (A) M0 macrophages were differentiated from THP-1 cells with various concentrations of PMA (***P<0.001, as compared with the THP-1 group; $^{###}$P<0.001, as compared with the 5 ng/ml PMA group). (B) RT-qPCR analysis of IL-10 expression in THP-1 cells with PMA and various concentrations of IL-4 (*P<0.05 and **P<0.01, as compared with the THP-1 group; $^{#}$P<0.05, $^{##}$P<0.01 and $^{###}$P<0.001, as compared with the M0 group; $^{&&&}$P<0.001, as compared with the IL-4 5 ng/ml group). (C) ELISA of IL-10 expression in THP-1 cells with PMA and various concentrations of IL-4 (***P<0.001, as compared with the THP-1 group; $^{###}$P<0.001, as compared with the M0 group). (D) RT-qPCR analysis of IL-12 expression in THP-1 cells with PMA and various concentrations of IFN-γ (*P<0.05 and **P<0.01, as compared with the THP-1 group; $^{#}$P<0.05, as compared with the M0 group). (E) RT-qPCR analysis of IL-12 expression in THP-1 cells with PMA, IFN-γ and various concentrations of LPS (***P<0.001, as compared with the THP-1 group; $^{###}$P<0.001, as compared with the M0 and 20 ng/ml IFN-γ group; $^{&}$P<0.05, as compared with the M0 in 20 ng/ml IFN-γ and 20 ng/ml LPS group). (F) ELISA of IL-12 expression in THP-1 cells with PMA, IFN-γ and various concentrations of LPS (*P<0.05 and **P<0.01, compared with the THP-1 group; $^{##}$P<0.01, as compared with the M0 and 20 ng/ml IFN-γ group). PMA, phorbol 12-myristate-13 acetate; LPS, lipopolysaccharide.

The results revealed that the expression of p-Rb/E2F1 proteins was significantly higher in the M2 macrophage group than in the other groups, although their expression decreased following treatment with BCG (Fig. 8A, E and F). iNOS (M1 marker) protein expression increased and ARG-1 (M2 marker) protein expression decreased in the BCG-induced M1 macrophage group compared with the M1 macrophage group (Fig. 8A-C). ARG-1 (M2 marker) protein expression decreased and iNOS

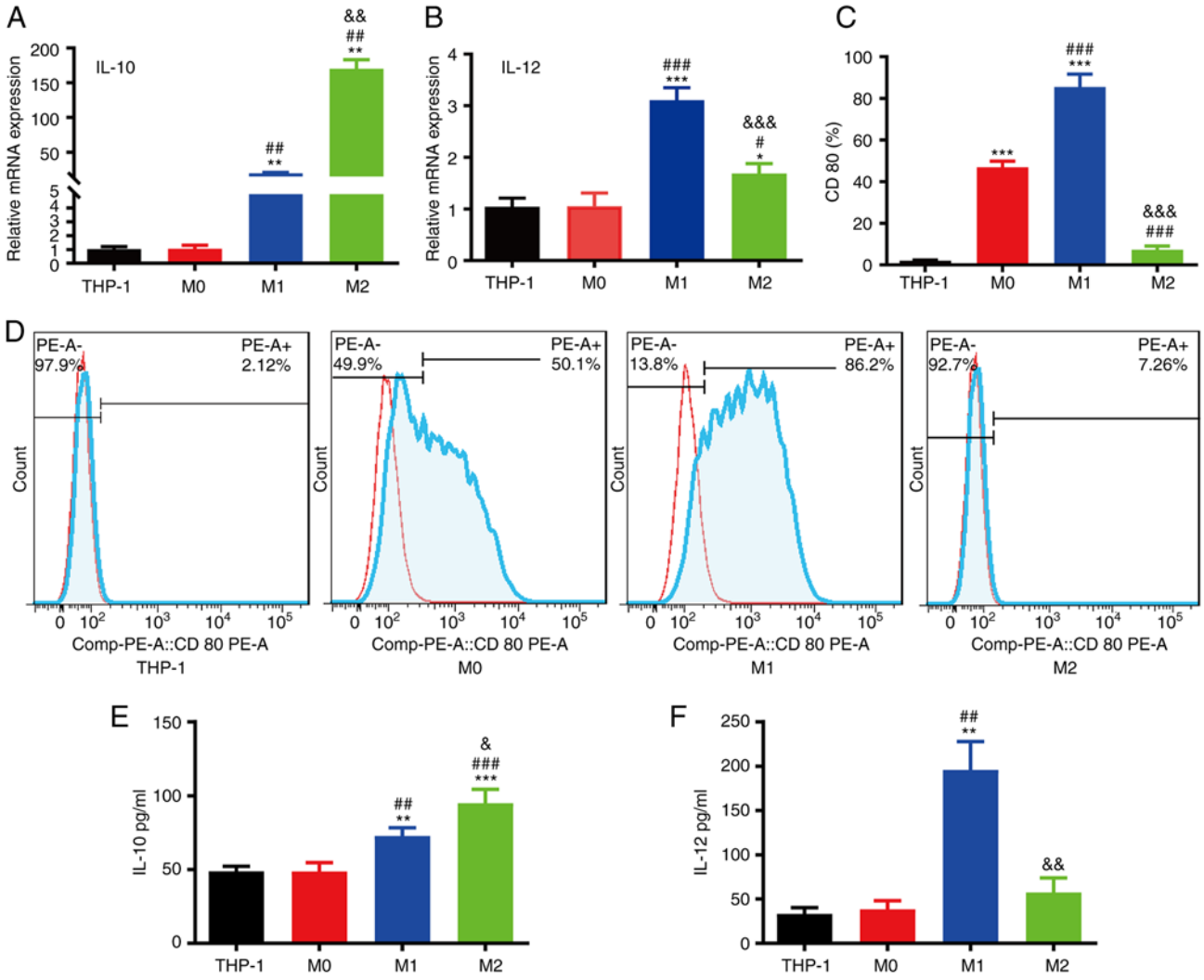

Figure 5. Characterization of macrophage polarization. (A) RT-qPCR analysis of IL-10 mRNA expression in the THP-1, M0, M1 and M2 groups. (B) RT-qPCR analysis of IL-12 mRNA expression in the THP-1, M0, M1 and M2 groups. (C) Quantification of CD80 in the THP-1, M0, M1 and M2 groups. (D) Flow cytometric analysis of CD80 protein expression in the THP-1, M0, M1 and M2 groups. (E) ELISA of IL-10 expression in the THP-1, M0, M1 and M2 groups. (F) ELISA of IL-12 expression in the THP-1, M0, M1 and M2 groups (*P<0.05, **P<0.01 and ***P<0.001, as compared with the THP-1 group; $^{\#}$P<0.05, $^{\#\#}$P<0.01 and $^{\#\#\#}$P<0.001, as compared with the M0 group; $^{\&}$P<0.05, $^{\&\&}$P<0.01 and $^{\&\&\&}$P<0.001, as compared with the M1 group).

(M1 marker) protein expression increased in the BCG-induced M2 macrophage group compared with the M2 macrophage group. The expression of the p53 protein was higher in M1/M2 macrophages with BCG than in those without BCG treatment (Fig. 8A and D).

Discussion

The tumour microenvironment (TME), which consists of fibroblasts, lymphatics, blood vessels, cells and inflammatory immune cells (36), plays a critical role in the progression of the occurrence, development, and prognosis of cervical cancer. TAMs are the main contributors to the TME via the accumulation and polarization of these cells. M1 macrophages, known as the 'fighting' macrophages, are tumoricidal directly via the excretion of pro-inflammatory cytokines, such as IL-6, IL-12, IL-23 and TNF-α (18), the depletion of the tumour stoma and their high antigen presentation capabilities (17). Therefore, these cells play a critical role in immune surveillance and are associated with a good prognosis in cancer (21,37). M1 macrophages are associated with the improved survival of patients with cervical cancer (38,39). The present study found that high transcriptional levels of IL-12 were significantly associated with a prolonged OS in patients with cervical cancer using the UALCAN and GEPIA databases. The results also demonstrated that IL-12, CD80 and iNOS were enriched in M1 macrophages, and M1 macrophages inhibited HeLa cell proliferation and promoted HeLa cell apoptosis. M2 macrophages, known as the 'aggressor' of tumours, may support tumour growth directly via the secretion of tumour-promoting cytokines and indirectly promote angiogenesis, cancer stem cells or the development of an immune-evasive microenvironment (40,41). The present study demonstrated that patients with cervical cancer with low transcriptional levels of IL-10 had a prolonged OS using the UALCAN, GEPIA and GSE databases. Moreover, it was confirmed that IL-10 and ARG expression was higher in the M2 macrophage group than in the M1 macrophage group.

Cervical cancer is closely related to a persistent infection of high-risk HPV. HPV vaccines are effective in preventing

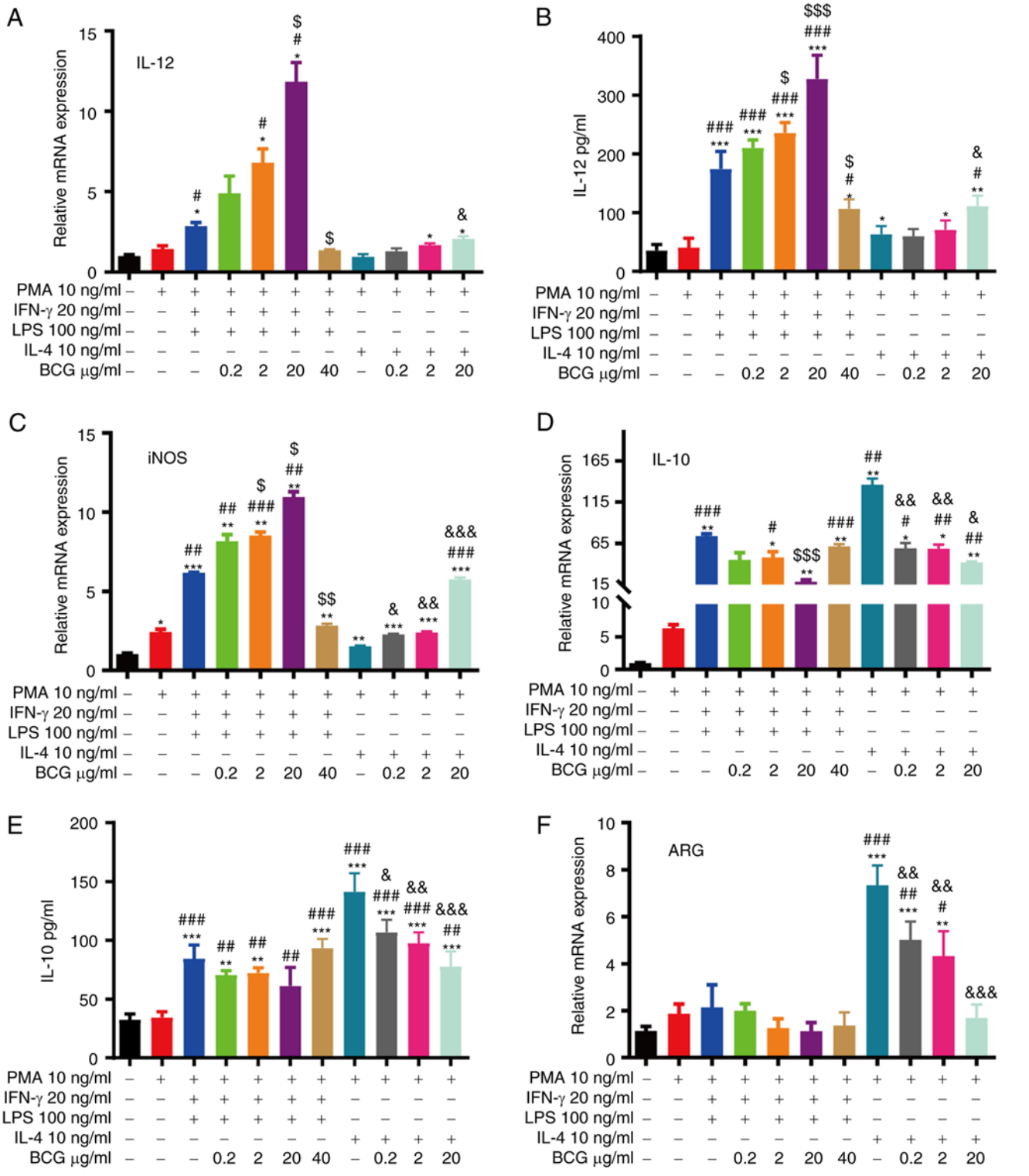

Figure 6. BCG promotes macrophage polarization towards the M1 phenotype and enhances the transition of M2 to M1 macrophages. RT-qPCR analysis of (A) IL-12, (C) iNOS, (D) IL-10 and (F) ARG mRNA expression in each group. ELISA of (B) IL-12 and (E) IL-10 expression in each group (*P<0.05, **P<0.01 and ***P<0.001, as compared with the THP-1 group; $^{\#}$P<0.05, $^{\#\#}$P<0.01 and $^{\#\#\#}$P<0.001, as compared with the M0 group; $^{\$}$P<0.05, $^{\$\$}$P<0.01 and $^{\$\$\$}$P<0.001, as compared with the M1 group; $^{\&}$P<0.05, $^{\&\&}$P<0.01 and $^{\&\&\&}$P<0.001, as compared with the M2 group). BCG, Bacillus Calmette-Guérin; iNOS, inducible nitric oxide synthase; ARG, arginase.

cervical cancer; however, these vaccines do not eliminate persistent HPV infections or prevent infected tissues from developing into malignant tumours (42). BCG has largely been used as a tuberculosis (TB) vaccine for 100 years (43). The intravesical treatment of BCG is the primary choice for treatment, and it has become the gold standard of immunotherapy for superficial bladder cancer (5,44). Immunostimulation with BCG markedly annihilates existing carcinoma *in situ* and suppresses the possibility of tumour progression or recurrence in treating bladder cancer, melanoma, kidney cancer, liver cancer,

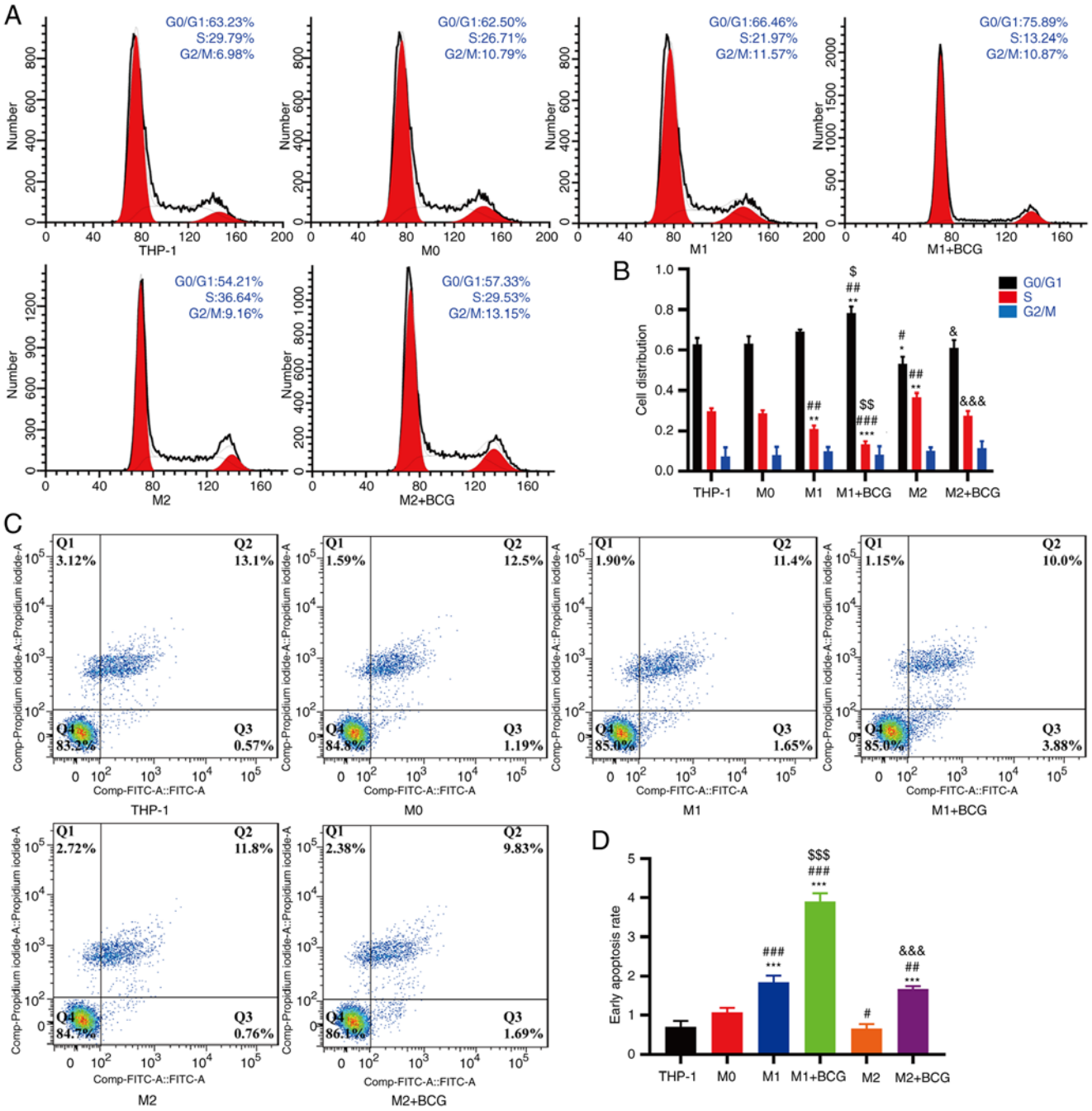

Figure 7. BCG inhibits cell proliferation and promotes the early apoptosis of M1/M2 macrophages in HeLa cells. (A) Flow cytometric analysis of the cell cycle in each group. (B) Cell distribution analysis results in each group. (C) Flow cytometric analysis of cell apoptosis in each group. (D) Early apoptosis of HeLa cell analysis in each group (*P<0.05, **P<0.01 and ***P<0.001, as compared with the THP-1 group; $^{\#}$P<0.05, $^{\#\#}$P<0.01 and $^{\#\#\#}$P<0.001, as compared with the M0 group; $^{\$}$P<0.05, $^{\$\$}$P<0.01 and $^{\$\$\$}$P<0.001, as compared with the M1 group; $^{\&}$P<0.05 and $^{\&\&\&}$P<0.001, as compared with M2 group). BCG, Bacillus Calmette-Guérin.

lymphoma, and acute leukaemia (45-47). The wide range of protection by BCG vaccine against non-associated pathogens and cancer to promote innate immunity and connect adaptive immune responses, stresses the urgent need to re-examine such microbe-based combination therapeutics for cancer treatment, particularly through local administration (48-50). BCG immunotherapy affects macrophage polarization in bladder carcinoma (51). In the present study, it was found that the levels of M1 markers, such as IL-12 and iNOS, were significantly increased in BCG-activated macrophages and that the levels of M2 markers, such as IL-10 and ARG, were decreased in BCG-activated macrophages. These results indicate that BCG promotes macrophage polarization toward the M1 phenotype and enhances the transition of M2 to M1 macrophages.

The molecular mechanism of HPV carcinogenesis is the integration of viral DNA into the chromosome of the host, and the E6 and E7 oncoproteins combine with the tumour suppressor genes, p53 and Rb, respectively, which leads to the inactivation of p53 and Rb, alterations in the cell cycle and DNA repair, and the progression of invasive cervical cancer (2,52). Rb is a key player in cell cycle regulation in which the tumour suppression function is inactivated via phosphorylation, and the tumour promotion function is inhibited via caspase cleavage (53). Rb inhibits cell proliferation by directly suppressing the

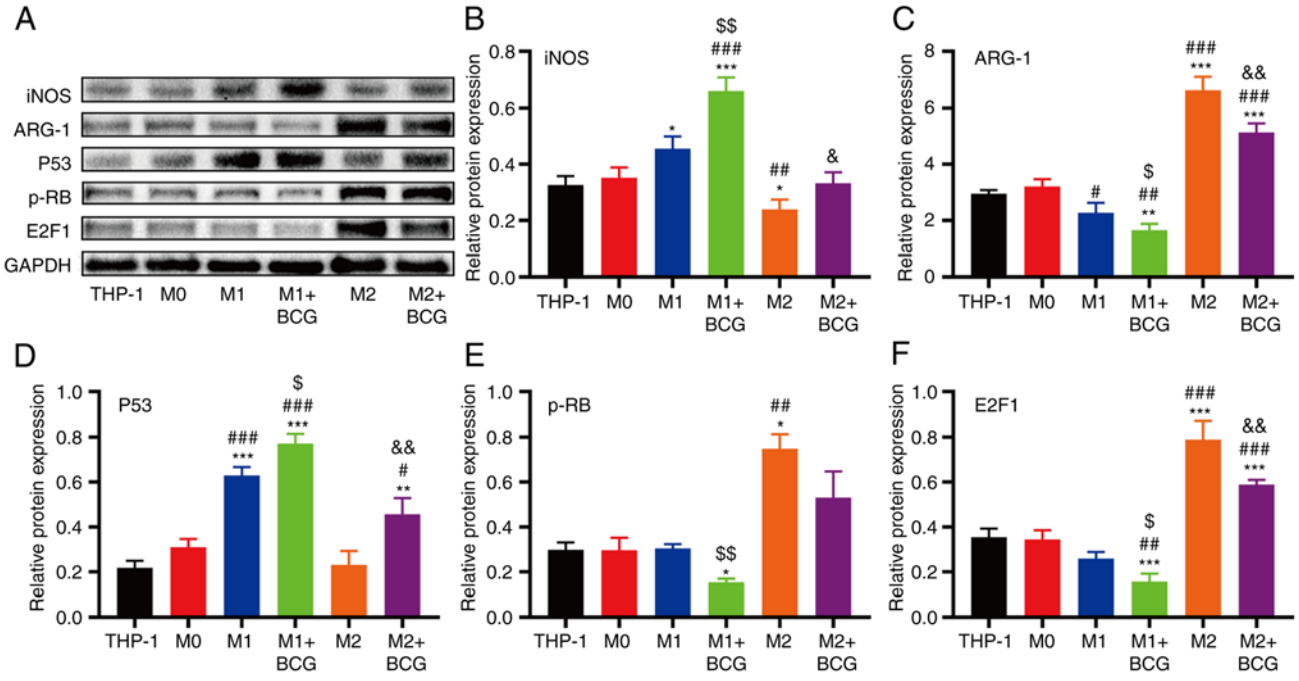

Figure 8. Effects of the Rb/E2F1 signalling pathway during BCG-induced M1/M2 macrophage activation. (A) Protein expression levels of iNOS, ARG-1, p53, p-Rb and E2F1 in each group were analysed using western blot analysis. Densitometric analysis results of (B) iNOS, (C) ARG-1, (D) p53, (E) p-Rb and (F) E2F1 expression (*P<0.05, **P<0.01 and ***P<0.001, as compared with the THP-1 group; $^{\#}$P<0.05, $^{\#\#}$P<0.01 and $^{\#\#\#}$P<0.001, as compared with the M0 group; $^{\$}$P<0.05 and $^{\$\$}$P<0.01, as compared with the M1 group; $^{\&}$P<0.05 and $^{\&\&}$P<0.01, as compared with the M2 group). BCG, Bacillus Calmette-Guérin; iNOS, inducible nitric oxide synthase; ARG-1, arginase; p-RB, retinoblastoma protein; E2F1, transcription factor E2F1.

transcription factor E2F1, which promotes cell growth, cell differentiation and DNA synthesis (54). The present study examined a series of DEGs associated with survival and identified the survival-based cell cycle, immune response and p53 signalling pathway in cervical cancer from the GEO database. The results revealed that the expression of p-Rb/E2F1 proteins was significantly higher in the M2 macrophage group than in the other groups and decreased after treatment with BCG.

In the present study, it was also demonstrated that BCG suppressed the activation of M2 macrophages by enhancing the proliferation of HeLa cells. It was also identified that M1 macrophages promoted apoptosis and that BCG further promoted the apoptosis of HeLa cells. These data suggest that BCG promotes the anti-tumour progression of M1 macrophages and inhibits the pro-tumour activation of M2 macrophages in HeLa cells. It was also found that BCG-induced M1/M2 macrophages influenced HeLa cell proliferation by increasing Rb/E2F1 expression.

In conclusion, the BCG vaccine has immunomodulatory properties that have recently been revealed (55). The findings of the present study provide valuable insight into the potential clinical therapeutic effects of BCG that may benefit patients with cervical cancer. BCG may prove to be an effective preventive measure for cervical cancer. Consequently, further experiments are needed to obtain a better understanding of the molecular mechanisms through which BCG regulates M1/M2 polarization and activates the cervical cancer microenvironment, and to confirm the findings presented herein.

Acknowledgements

The authors would like to thank Dr Taoliang Chen and Dr Weimin Huang for their insightful discussions with the present study. The authors would also thank Professor Linlang Guo (Department of Pathology, Zhujiang Hospital, Southern Medical University, Shenzhen, China) for editing this manuscript.

Funding

The present study was supported by grants from the Shenzhen Science and Technology Innovation Committee (nos. JCYJ20160427190929616 and JCYJ20170307091700193) and the Shenzhen San Ming Project of Medicine (no. SZSM 201612042).

Availability of data and materials

The datasets used and/or analysed during the current study are available from the corresponding author upon reasonable request.

Authors' contributions

ZL, LL, HH and KL designed the experiments. LL, WS and XX performed the experiments. LL, XW and SY performed the statistical analyses. LL wrote the first draft of the manuscript, and all authors commented on the subsequent drafts. ZL and LL reviewed the final draft and confirmed the authenticity of all the raw data. All authors have read and approved the final manuscript.

Ethics approval and consent to participate

Not applicable.

Patient consent for publication

Not applicable.

Competing interests

The authors declare that they have no competing interests.

References

1. Bray F, Ferlay J, Soerjomataram I, Siegel RL, Torre LA and Jemal A: Global cancer statistics 2018: GLOBOCAN estimates of incidence and mortality worldwide for 36 cancers in 185 countries. CA Cancer J Clin 68: 394-424, 2018.
2. Cancer Genome Atlas Research Network, Albert Einstein College of Medicine, Analytical Biological Services, Barretos Cancer Hospital, Baylor College of Medicine, Beckman Research Institute of City of Hope; Buck Institute for Research on Aging; Canada's Michael Smith Genome Sciences Centre; Harvard Medical School, Helen F, *et al*: Integrated genomic and molecular characterization of cervical cancer. Nature 543: 378-384, 2017.
3. Mossanen M and Gore JL: The burden of bladder cancer care: Direct and indirect costs. Curr Opin Urol 24: 487-491, 2014.
4. Gandhi NM, Morales A and Lamm DL: Bacillus Calmette-Guerin immunotherapy for genitourinary cancer. BJU Int 112: 288-297, 2013.
5. Kiselyov A, Bunimovich-Mendrazitsky S and Startsev V: Treatment of non-muscle invasive bladder cancer with Bacillus Calmette-Guerin (BCG): Biological markers and simulation studies. BBA Clin 4: 27-34, 2015.
6. Pichler R, Borena W, Schäfer G, Manzl C, Culig Z, List S, Neururer S, Von Laer D, Heidegger I, Klocker H, *et al*: Low prevalence of HPV detection and genotyping in non-muscle invasive bladder cancer using single-step PCR followed by reverse line blot. World J Urol 33: 2145-2151, 2015.
7. Metawea B, El-Nashar AR, Kamel I, Kassem W and Shamloul R: Application of viable bacille Calmette-Guerin topically as a potential therapeutic modality in condylomata acuminata: A placebo-controlled study. Urology 65: 247-250, 2005.
8. Fayed ST, Amer M, Ammar E and Salam MA: Local BCG injection administered to patients with flat condyloma of the cervix. Int J Gynaecol Obstet 107: 253-254, 2009.
9. Böhle A, Büttner H and Jocham D: Primary treatment of condylomataacuminata with viable bacillus Calmette-Guerin. J Urol 165: 834-836, 2001.
10. Cappello F: Effect of of cervical antitumoral immunity activation on CIN. Minerva Ginecol 43: 405-408, 1991 (In Italian).
11. Lu X, Wu L, Liu Z, Xie L and Wang S: Peripheral blood mononuclear cells inhibit proliferation and promote apoptosis of HeLa cells following stimulation with Bacillus Calmette-Guerin. Exp Ther Med 5: 561-566, 2013.
12. Sonoda T, Sugimura K, Ikemoto SI, Kawashima H and Nakatani T: Significance of target cell infection and natural killer cells in the anti-tumor effects of bacillus Calmette-Guerin in murine bladder cancer. Oncol Rep 17: 1469-1474, 2007.
13. Piaggio F, Kondylis V, Pastorino F, Di Paolo D, Perri P, Cossu I, Schorn F, Marinaccio C, Murgia D, Daga A, *et al*: A novel liposomal Clodronate depletes tumor-associated macrophages in primary and metastatic melanoma: Anti-angiogenic and anti-tumor effects. J Control Release 223: 165-177, 2016.
14. Geissmann F, Manz MG, Jung S, Sieweke MH, Merad M and Ley K: Development of monocytes, macrophages, and dendritic cells. Science 327: 656-661, 2010.
15. Mantovani A, Sozzani S, Locati M, Allavena P and Sica A: Macrophage polarization tumor-associated macrophages as a paradigm for polarized M2 mononuclear phagocytes. Trends Immunol 11: 23, 2002.
16. Sica A and Mantovani A: Macrophage plasticity and polarization: In vivo veritas. J Clin Invest 122: 787-795, 2012.
17. Biswas SK and Mantovani A: Macrophage plasticity and interaction with lymphocyte subsets: Cancer as a paradigm. Nat Immunol 11: 889-896, 2010.
18. Zheng X, Turkowski K, Mora J, Brüne B, Seeger W, Weigert A and Savai R: Redirecting tumor-associated macrophages to become tumoricidal effectorsas a novel strategy. Oncotarget 29: 48436-48452, 2017.
19. Liu Q, Tian Y, Zhao X, Jing H, Xie Q, Li P, Li P, Li D, Yan D and Zhu X: NMAAP1 expressed in BCG-activated macrophage promotes M1 macrophage polarization. Mol Cells 38: 886-894, 2015.
20. van Dalen FJ, van Stevendaal M, Fennemann FL, Verdoes M and Ilina O: Molecular repolarisation of tumour-associated macrophages. Molecules 24: 9, 2018.
21. Mills CD: M1 and M2 macrophages: Oracles of health and disease. Crit Rev Immunol 32: 463-488, 2012.
22. Schiffman M, Doorbar J, Wentzensen N, de Sanjose S, Fakhry C, Monk BJ, Stanley MA and Franceschi S: Carcinogenic human papillomavirus infection. Nat Rev Dis Primers 2: 16086, 2016.
23. de Martel C, Plummer M, Vignat J and Franceschi S: Worldwide burden of cancer attributable to HPV by site, country and HPV type. Int J Cancer 141: 664-670, 2017.
24. Stevanovic S, Draper LM, Langhan MM, Campbell TE, Kwong ML, Wunderlich JR, Dudley ME, Yang JC, Sherry RM, Kammula US, *et al*: Complete regression of metastatic cervical cancer after treatment with human papillomavirus-targeted tumor-infiltrating T cells. J Clin Oncol 33: 1543-1550, 2015.
25. Seiwert TY, Burtness B, Mehra R, Weiss J, Berger R, Eder JP, Heath K, McClanahan T, Lunceford J, Gause C, *et al*: Safety and clinical activity of pembrolizumab for treatment of recurrent or metastatic squamous cell carcinoma of the head and neck (KEYNOTE-012): An open-label, multicentre, phase 1b trial. Lancet Oncol 17: 956-965, 2016.
26. Morris VK, Salem ME, Nimeiri H, Iqbal S, Singh P, Ciombor K, Polite B, Deming D, Chan E, Wade JL, *et al*: Nivolumab for previously treated unresectable metastatic anal cancer (NCI9673): A multicentre, single-arm, phase 2 study. Lancet Oncol 18: 446-453, 2017.
27. van der Burg SH and Melief CJ: Therapeutic vaccination against human papilloma virus induced malignancies. Curr Opin Immunol 23: 252-257, 2011.
28. Stevanovic S, Pasetto A, Helman SR, Gartner JJ, Prickett TD, Howie B, Robins HS, Robbins PF, Klebanoff CA, Rosenberg SA and Hinrichs CS: Landscape of immunogenic tumor antigens in successful immunotherapy of virally induced epithelial cancer. Science 356: 200-205, 2017.
29. Tang Z, Li C, Kang B, Gao G, Li C and Zhang Z: GEPIA: A web server for cancer and normal gene expression profiling and interactive analyses. Nucleic Acids Res 45: W98-W102, 2017.
30. Chandrashekar DS, Bashel B, Balasubramanya SAH, Creighton CJ, Ponce-Rodriguez I, Chakravarthi B and Varambally S: UALCAN: A portal for facilitating tumor subgroup gene expression and survival analyses. Neoplasia 19: 649-658, 2017.
31. Huang DW, Sherman BT and Lempicki RA: Systematic and integrative analysis of large gene lists using DAVID bioinformatics resources. Nat Protoc 4: 44-57, 2009.
32. Franceschini A, Szklarczyk D, Frankild S, Kuhn M, Simonovic M, Roth A, Lin J, Minguez P, Bork P, von Mering C and Jensen LJ: STRING v9.1: Protein-protein interaction networks, with increased coverage and integration. Nucleic Acids Res 41: D808-D815, 2012.
33. Livak KJ and Schmittgen TD: Analysis of relative gene expression data using real-time quantitative PCR and the 2(-Delta Delta C(T)) method. Methods 25: 402-408, 2001.
34. Liu H, Zhang L and Wang P: Complement factor H-related 3 overexpression affects hepatocellular carcinoma proliferation and apoptosis. Mol Med Rep 20: 2694-2702, 2019.
35. Sánchez-Rodríguez C, Cruces KP, Ayora JR, Martín-Sanz E and Sanz-Fernández R: BCG immune activation reduces growth and angiogenesis in an in vitro model of head and neck squamous cell carcinoma. Vaccine 35: 6395-6403, 2017.
36. Greten FR and Grivennikov SI: Inflammation and cancer: Triggers, mechanisms, and consequences. Immunity 51: 27-41, 2019.
37. Honkanen TJ, Tikkanen A, Karihtala P, Mäkinen M, Väyrynen JP and Koivunen JP: Prognostic and predictive role of tumour-associated macrophages in HER2 positive breast cancer. Sci Rep 9: 10961, 2019.
38. Yang M, McKay D, Pollard JW and Lewis CE: Diverse functions of macrophages in different tumor microenvironments. Cancer Res 78: 5492-5503, 2018.
39. de Vos van Steenwijk PJ, Ramwadhdoebe TH, Goedemans R, Doorduijn EM, van Ham JJ, Gorter A, van Hall T, Kuijjer ML, van Poelgeest MIE, van der Burg SH and Jordanova ES: Tumor-infiltrating CD14-positive myeloid cells and CD8-positive T-cells prolong survival in patients with cervical carcinoma. Int J Cancer 133: 2884-2894, 2013.

40. Jayasingam SD, Citartan M, Thang TH, Zin AA, Ang KC and Ch'ng ES: Evaluating the polarization of tumor-associated macrophages into M1 and M2 phenotypes in human cancer tissue: Technicalities and challenges in routine clinical practice. Front Oncol 9: 1512, 2019.
41. Mantovani A, Marchesi F, Malesci A, Laghi L and Allavena P: Tumour-associated macrophages as treatment targets in oncology. Nat Rev Clin Oncol 14: 399-416, 2017.
42. English PMB: Eradicating cervical cancer is unlikely. BMJ 366: l4953, 2019.
43. Luca S and Mihaescu T: History of BCG vaccine. Maedica (Bucur) 8: 53-58, 2013.
44. Locht C and Lerm M: Good old BCG-what a century-old vaccine can contribute to modern medicine. J Intern Med 12: 611-613, 2020.
45. Mustafa AS: BCG as a vector for novel recombinant vaccines against infectious diseases and cancers. Vaccines (Basel) 84: 736, 2020.
46. Xue QJ, Li YQ, Yang CQ, Chen T, Li XZ, Cheng B and Wang CM: Anti-tumour research of recombinant BCG using BZLF1 and hGM-CSF fusion genes.Vaccine 14: 1599-1607, 2017.
47. Kremenovic M, Schenk M and Lee DJ: Clinical and molecular insights into BCG immunotherapy for melanoma. J Intern Med 288: 625-640, 2020.
48. Koti M, Morales A, Graham CH and Siemens DR: BCG vaccine and COVID-19: Implications for infection prophylaxis and cancer immunotherapy. J Immunother Cancer 8: e001119, 2020
49. Usher NT, Chang S, Howard RS, Martinez A, Harrison LH, Santosham M and Aronson NE: Association of BCG vaccination in childhood with subsequent cancer diagnoses A 60-year follow-up of a clinical trial. JAMA Netw Open 2: e1912014, 2019.
50. Jabbar IA, Fernando GJ, Saunders N, Aldovini A, Young R, Malcolm K and Frazer IH: Immune responses induced by BCG recombinant for human papillomavirus L1 and E7 proteins. Vaccine 18: 2444-2453, 2000.
51. Svatek RS, Zhao XR, Morales EE, Jha MK, Tseng TY, Hugen CM, Hurez V, Hernandez J and Curiel TJ: Sequential intravesical mitomycin plus Bacillus Calmette-Guerin for non-muscle-invasive urothelial bladder carcinoma: Translational and phase I clinical trial. Clin Cancer Res 21: 303-311, 2015.
52. Doorbar J, Egawa N, Griffin H, Kranjec C and Murakami I: Human papillomavirus molecular biology and disease association. Rev Med Virol 25 (Suppl 1): S2-S23, 2015.
53. Borges HL, Bird J, Wasson K, Cardiff RD, Varki N, Eckmann L and Wang JY: Tumor promotion by caspase-resistant retinoblastoma protein. Proc Natl Acad Sci 102: 15587-15592, 2005.
54. van den Heuvel S and Dyson NJ: Conserved functions of the pRB and E2F families. Nat Rev Mol Cell Biol 9: 713-724, 2008.
55. Yamazaki-Nakashimada MA, Unzueta A, Gámez-González LB, González-Saldaña N and Sorensen RU: BCG: A vaccine with multiple faces. Hum Vaccin Immunother 16: 1841-1850, 2020.